FLUX DISTRIBUTION AND FIELD ANALYSIS OF CSP COLLECTOR

K. S. Reddy*, Veershetty Gumtapure

Heat Transfer and Thermal Power Laboratory,

Department of Mechanical Engineering

Indian Institute of Technology Madras, Chennai-600036, India

* Email: ksreddy@iitm.ac.in (K. S. Reddy), Tel.: +91-44-22574702, Fax: +91-44-22574652

Abstract

The flux distribution on the focal plane of the receiver and spacing of parabolic dish collector arrays for power generation are investigated in this paper. The mathematical models are developed to study the variation in the image size on the receiver and thereby flux distribution on the focal plane. The effect of focal image dispersion characteristics on the receiver is studied with respect to rim angle. It is observed that the focal image size is very small for 40^o to 50^o rim angle. The optimum space required between the dishes is investigated for deployment of power generation. The area covered and orientation of shadows depends on time of the day, latitude of the place and declination. To compute the minimum distance required between the dishes, a year round shadow analysis of dish collectors is performed for different arrangement of the dish collector. Ground utilization factor (ratio of total collector area to land area) determines the fraction of solar energy actually used out of the total energy received by the land area. A year round shadow profile of dish collector is to arrive minimum spacing between the dishes to avoid shadowing. In-line arrangement of the solar dish collectors is found to be a better choice in terms of the minimum land area required. The spacing between the dishes in east–west direction is chosen such a way that it is equal to shadow length for a given operating hours after the sunrise at solar azimuth angle of 90°. In north–south direction, the spacing distance is equal to shadow length at noon at a declination of -23.45°. The generalized correlations are developed for both east-west and north-south spacing distances as the function of latitude and plant operating hours.

Key words: Solar parabolic dish, Flux distribution, Spacing distance, Shadow profile, Land use factor

1. Introduction

The concentrating solar thermal technologies are one of the most effective ways of collecting solar energy. Concentrating solar power systems use lenses or mirrors combined with tracking systems to focus sunlight on focal plane where receiver is kept and the resulting heat is absorbed by a heat transfer fluid and used for further applications. The primary mechanisms for concentrating sunlight are the linear Fresnel reflectors, parabolic trough, power tower and parabolic dish. The concentrated solar radiation is to be converted into high-temperature heat with an effective receiver design with minimum heat loss. The performance of the large scale solar power plant depends mainly on the flux distribution on the receiver and shadow falling on the reflecting surfaces by adjacent collector. Several attempts have been made to calculate the flux distribution on receiver. Robert et al., (1957) carried out the theoretical investigation of flux distribution on focal plane of dish system assuming the sun disk's of uniform intensity. Jeter (1986) presented the procedure for calculating the distribution of concentrated flux in parabolic collector. The procedure was based on the concepts of flux integral and radiant intensity and the collector was assumed to be operating with zero pointing error. Kaushika (1993) presented characteristics relevant to the design and cost consideration of the multifaceted dish collector. Kaushika and Reddy (2000) investigated the flux distribution in a low cost paraboloidal dish receiver and also determined stagnation temperature at focal point experimentally. Liul et al., (2003) performed an error analysis for flux distribution on a receiver surface. Aparporn and Somchai (2007) estimated flux distribution analysis on central receiver system. Reddy and Veershetty (2009) developed a model for the flux distribution in the focal plane for a parabolic dish concentrator. This model is used for estimating the image size and flux distribution at focal plane for fuzzy focal solar dish concentrator.

Barra et al., (1977) presented an analytical - numerical method for evaluating the shading effect in a typical solar power plant of concentrating cylindrical parabolic collectors tracking the sun. Appelbaum and Bany (1979) analysed the shading of vertical and inclined poles and collectors. This information was used for optimal development of collectors in a given area which includes the tilt angle, collector size, spacing between the collectors and number of rows. Groumpos and Khouzam (1987) presented a generic mathematical framework for the analysis of the shadow effect of large solar collector power system for three possible orientations: fixed tilt, full tracking and half tracking. It has been found that full tracking collectors requires more spacing between them than half tracking and fixed collectors. Aronova et al., (2008) developed a numerical model for determining the energy generated by tracking photoelectric power modules with partial shadowing. They have studied how shadowing influences the relative annual losses of the power generated by the modules, and arrived at optimum arrangement of the module at any chosen place with minimum losses. There is not much analysis has done for shadowing effect on power generation for two axis tracking concentrating system specially parabloic dish collector. In this article an attempt has been made to analyse the spacing between the dish arrays and shadowing effect on adjacent dishes.

2. Mathematical modelling for flux distribution and dish collector field analysis

The concentrated solar radiation flux is usually distributed non-uniformly over the receiver surface; therefore the calculation of the local flux concentration ratio is often difficult. The aim of this work is to investigate the flux distribution on the receiver plane for the solar dish collector and dish collector field analysis. A receiver placed at the focal point of the parabola intercepts all the solar rays reflected by the dish reflector surface as shown in Fig.1 and hence high intensity of radiation is available at the receiver that can be used as a high temperature heat source for power generation. A typical layout of the solar parabolic dish power plant is shown in Fig. 2. The collector field consists of an array of solar parabolic dish collectors placed in east-west as well as north-south direction. The solar to electrical energy conversion depends on the availability of the direct solar irradiation, optimum spacing of the dish arrays and operating hours. The optimum spacing between the dishes must be chosen in such a way that the shadow of the dishes does not fall on the adjacent dishes at any point of time during a year.

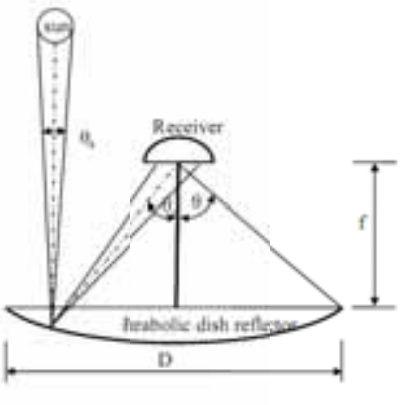

Fig. 1: Solar parabolic dish collector configuration

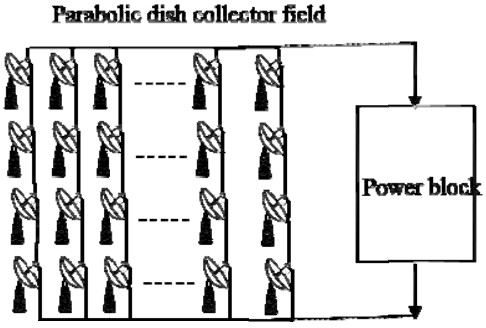

Fig. 2: Parabolic dish power plant layout

2.1 Image formation on the dish receiver

Consider a parabolic dish concentrator as shown in Fig.1 for analysing the image formation at the focal plane. For a given aperture diameter, the focal distance 'f' of the concentrator and its curvature depends on the rim angle of the dish. The equation of the surfaces of the parabola with respect to their own axis is of the form:

$$y = \frac{x^2}{4f} \qquad \text{(eq.1)}$$

Focal length is related to the aperture radius 'R' and half rim angle 'θ' as:

$$f = \frac{R\sin\theta}{2(1-\cos\theta)} \quad \text{(eq. 2)}$$

Elliptical images are formed on the horizontally placed receiver, because of the conical nature of the sun's rays (θ_s=32'). The width of the receiver can be fixed based on the major axis length of the elliptical images formed. The semi major length of the elliptical image is given by:

$$a = \frac{2f\tan\theta_s}{\cos\theta(1+\cos\theta)} \quad \text{(eq. 3)}$$

The minor axis length of the elliptical image is given by

$$b = a.\cos\theta \quad \text{(eq. 4)}$$

The size of the image at the focal plane is twice the semi-major axis of the ellipse and is given as :

$$2a = \frac{4f.\tan\theta_s}{\cos\theta(1+\cos\theta)} \quad \text{(eq. 5)}$$

Area of the image at the focal spot is expressed as:

$$A_i = \frac{4\pi f^2.\tan^2\theta_s}{\cos^2\theta(1+\cos\theta)^2} \quad \text{(eq. 6)}$$

Aperture area of the dish reflector is given as:

$$A_p = 4\pi f^2.\tan^2(\theta/2) \quad \text{(eq. 7)}$$

Concentration ratio of the dish system is expressed as:

$$\frac{A_p}{A_i} = \frac{\sin^2\theta.\cos^2\theta}{\tan^2\theta_s} \quad \text{(eq. 8)}$$

2.2 Shadow around solar parabolic dish collector

The shadow length of the parabolic dish collector depends on the latitude of the place, declination and sun altitude angle. The shadow length of the parabolic dish concentrator may be expressed as:

$$L_{sh} = \frac{D}{\sin\alpha} \quad \text{(eq. 9)}$$

The sun altitude angle (α) is given as:

$$\sin\alpha = \sin\phi.\sin\delta + \cos\phi.\cos\delta.\cos\omega \quad \text{(eq. 10)}$$

The declination angle is given as:

$$\delta = 23.45\sin\left[\frac{360}{365}(284+n)\right] \quad \text{(eq.11)}$$

The sunrise or sunset hour angles are obtained by setting the α = 0 in eq. (10) and expressed as:

$$\cos\omega_{sr} = (-\tan\phi.\tan\delta) \quad \text{(eq. 12)}$$

At any given solar altitude angle, the shadow cast by the dish on plain ground is in the form of ellipse except for the altitude angle 90°, where the shadow is circular equal to diameter and at bottom of the dish. The

length of major axis of the ellipse is equal to the shadow length and length of minor axis is equal to the diameter of the dish, if the dish is perfectly tracking the sun.

The orientation of the shadow around the dish depends on solar azimuth angle, which is expressed as:

$$\cos\gamma_s = \left(\frac{\sin\alpha.\sin\phi - \sin\delta}{\cos\alpha.\cos\phi}\right) \quad \text{(eq. 13)}$$

2.3 Positioning of the parabolic dish collector field and land use factor

The arrangement of the dish arrays are made in such a way that the land area required to arrange the dishes must be as small as possible without the shadow falling on the any of the surrounding dishes at any time of the operation in a day throughout the year. The spacing between the dishes in east-west direction must be equal to the extreme shadow length at that operating hour to avoid the shadow falling on the adjacent dish. The minimum shadow length will occur in east-west direction when the solar azimuth angle is 90° for given operating hours on a particular day. Therefore, it is required to determine the declination (day of the year) on which the azimuth angle is 90° for given operating hours to determine the minimum shadow length in east-west direction. Equations (10), (12) and (13) are used to evaluate the declination at which the azimuth angle is 90° for given operating hours and we get,

$$\tan\delta = -\cot\phi.\cos\{\tan^{-1}[-\cot^2\phi.\mathrm{cosec}\,\omega_x - \cot\omega_x]\} \quad \text{(eq. 14)}$$

The solar altitude angle at which the azimuth angle is 90° for given operating hours can be expressed as:

$$\sin\alpha|_{\gamma_s=90^o} = \sin\phi.\sin(\tan^{-1}Y) + \cos\phi.\cos(\tan^{-1}Y).\cos(\tan^{-1}X - \omega_x) \quad \text{(eq. 15)}$$

where,

$$X = \left(-\cot^2\phi.\cos ec\,\omega_x - \cot\omega_x\right)$$

$$Y = -\cot\phi.\cos(\tan^{-1}X)$$

Shadow length in east-west direction at azimuth angle 90° is expressed as:

$$L_{sh\_EW} = \frac{D}{\sin\alpha|_{\gamma_s=90^o}} \quad \text{(eq. 16)}$$

The spacing in north-south direction is chosen in such a way that the shadow does not fall on the adjacent dish at noon in any of day throughout the year. In order to avoid the shadow falling on the adjacent dish at noon, the spacing distance between the dishes is taken as maximum shadow length which occurs on the declination -23.45°. For maximum shadow at noon, ω = 0° and δ = -23.45°. From eq. (10) the solar altitude angle is expressed as:

$$\sin\alpha|_{\delta=-23.45^o} = \sin\phi.\sin\delta + \cos\phi.\cos\delta \quad \text{(eq. 17)}$$

The shadow length in north-south direction at noon:

$$L_{sh\_NS} = \frac{D}{\sin\alpha|_{\delta=-23.45^o}} \quad \text{(eq. 18)}$$

Land area required around the dish, is the product of the spacing distances in east-west direction and north-south direction for given operating hours and is expressed as:

$$A_{land} = \frac{D^2}{\sin\alpha|_{\gamma_s=90^o} \times \sin\alpha|_{\delta=-23.45^o}} \quad \text{(eq. 19)}$$

Land use factor (LUF) is the ratio of the land around the dish to the aperture area of the dish which is given by:

$$LUF = \frac{A_{land}}{A_p} = \frac{4}{\pi(\sin\alpha|_{\gamma=90^o} \times \sin\alpha|_{\delta=-23.45^o})} \quad \text{(eq. 20)}$$

2.4 Shadow effect on the adjacent dishes

The shadow of the dish on the adjacent dishes has been estimated. If the dish system operating hour and the east-west direction spacing distance between the dishes is same, shadow will touch bottom tip of the adjacent dish. If the dish system operates earlier than this hour, the shadow will fall on the adjacent dishes as shown in Fig. 3. When dishes are viewed in the direction of the sunrays, on plane perpendicular to the sun rays (X-X′ plane) they look like two circles just touching each other if the operating and spacing distance selection timing are same, whereas if the operating time is earlier than the spacing distance selection time they look like two circles overlapping on each other.

The shadow covered on the adjacent dish (area intersection of the two circles) can be expressed as:

$$A_{sh} = \frac{D^2}{2}\cos^{-1}\left(\frac{d}{D}\right) - \frac{d}{2}\sqrt{D^2 - d^2} \quad \text{(eq. 21)}$$

where, d = distance between the centre of the dishes as viewed parallel to sunrays, when dishes are perfectly focused to sun. The value of'd' depends on the solar elevation angle, solar azimuth angle and positioning of the dish with respect to the other dish on which shadow is falling on it.

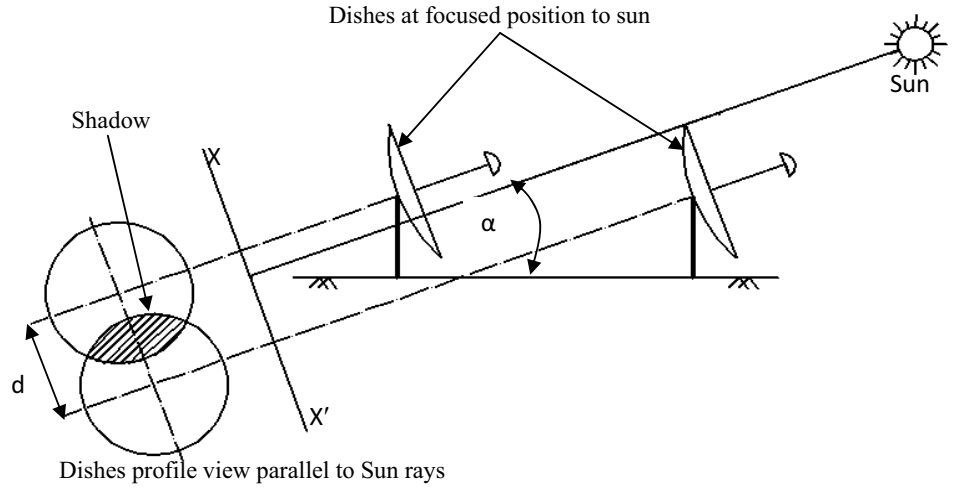

Fig. 3: Shadow falling on the adjacent dish operating at earlier than spacing setting hour

3. Results and Discussion

3.1. Image formation and local concentration at receiver

The super imposition of number of elliptical images with radial distance from target centre is shown in Fig.4. Maximum concentration ratio exists at the centre as all the images formed overlap in the central region and the concentration ratio decreases on moving away from the centre. The effect of the rim angle on the image formed at focal plane by solar dish concentrator has been studied and is shown in Fig. 5. The concentration ratio can be calculated by taking the ratio of the aperture area of the concentrator to image area at the focal plane. It can be seen that the concentration ratio is maximum for rim angles about 45^o.

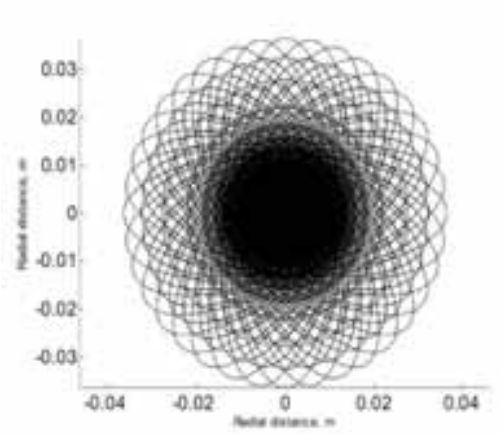

Fig. 4: Image formed on the receiver

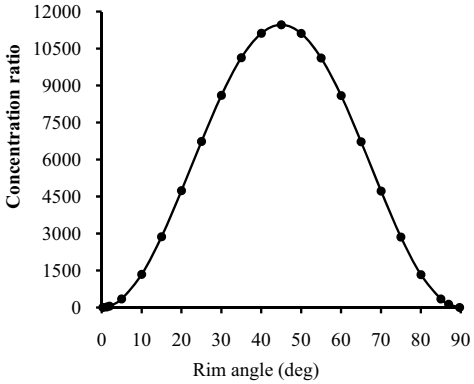

Fig. 5: Concentration ratio as a function of rim angle

3.2 Shadow profile, positioning of the dishes and land utilization

To determine shadow profile around the dish for any operating time throughout the year, MATLAB code has been developed. To illustrate how shadow profile occurs around the dish throughout the year, two extreme latitudes of India say 8°N and 35°N are considered, operating from 2 hours after sunrise to 2 hours before sunset is shown in Fig. 6. Each ellipse on west side represents the shadow profile for dish system operating at 2 hours after sunrise. When the dish is set to operate at 2 hours after sunrise, the shadow length will be maximum and as time progresses the shadow length decreases receding towards the dish. The top most ellipses correspond to the shadow of the dish for the declination -23.45°, whereas bottom most ellipses is for the declination +23.45° and in-between ellipses correspond to other declinations. The similar shadow profile will occur on east side at 2 hours before sunset. The shadow length will be longer at noon time for the declination -23.45° than the declination +23.45°.

The shadow profile around the dish throughout the year depends on the latitude, operating hour, declination and azimuth angle. The shadow length shown in Fig.6 is in non-dimensional form and expressed as the ratio of shadow length to the diameter of the dish (L_{sh}/D). The position of the dish is shown as the filled circle at the centre (only horizontal position) whose size is equal to its diameter. It is observed that at higher latitude, the shadow profile is larger as compared to that of lower latitude places for the same operating hours. If the system operates in the early hours of the sunrise, the shadow cast by the dish is very large as solar altitude angle is low as compared to later hours. This shadow profile is useful in selecting optimum spacing between the dish arrays without shadow falling on any adjacent dishes in any day of the year.

The arrangement of the dish arrays for latitudes 8°N and 35°N operating from 2 hours after sunrise to 2 hours before sunset are shown in Fig. 7. The dish (D_R) is taken as reference to locate other dishes around it. The dishes D_E, D_R and D_W are arranged in-line with spacing distance equal to the shadow length at 2 hours after sunrise in east-west direction. The dishes D_N, D_R and D_S are arranged in-line with spacing distance equal to the shadow length at noon at declination -23.45^o in north-south direction. The corner dishes (D_{NE}, D_{SE}, D_{NW} and D_{SW}) are arranged such a way that they are in-line with respect to the adjacent dishes in east-west or north-south direction spacing distance equal to shadow length in respective direction. The variation of the spacing in east-west direction for the latitudes ranging from 8°N to 35°N and operating hours ranging from half an hour to 2.5 hours is shown in Fig.8. The spacing between the dishes in east-west direction for latitudes 8°N and 35°N, operating after half an hour and 2.5 hours after sunrise are found as 7.74D and 1.66D; 9.41D and 1.97D of the dish, respectively.

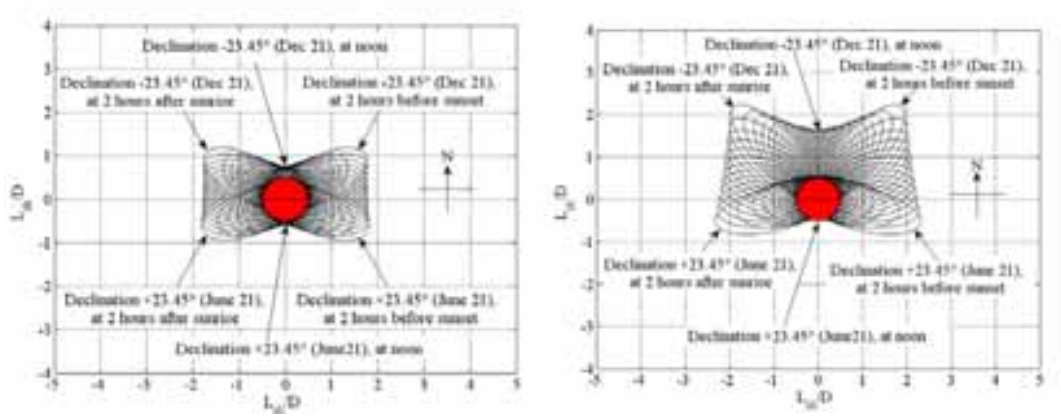

(a) (b)

Fig. 6: Shadow profile around the dish operating from after 2 hrs sunrise to 2 hrs before sunset at latitudes (a) 8°N and (b) 35°N

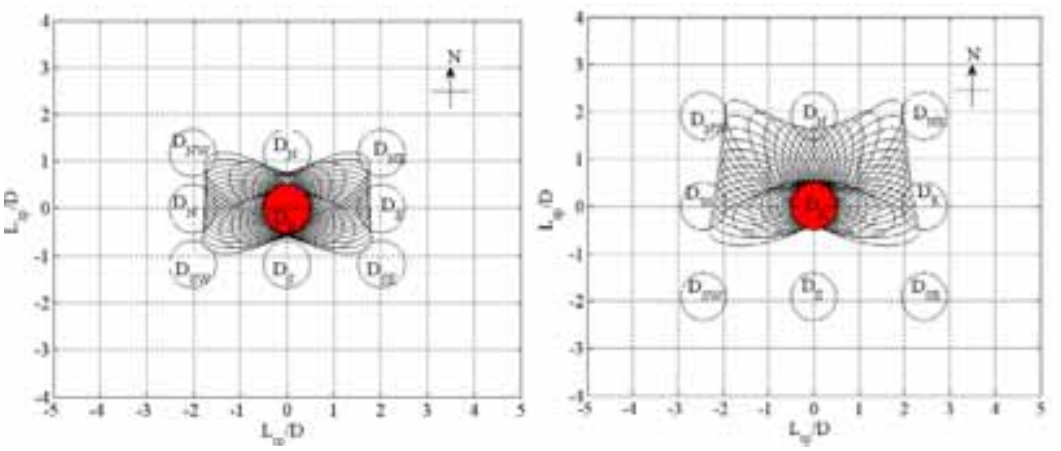

(a) (b)

Fig. 7: Spacing distance between the dishes after 2 hours sunrise and 2 hours before sunset at latitudes (a) 8°N and (b) 35° N

The generalized correlation has been developed to calculate the spacing between the dishes in east-west direction as the function of operating hours (t) and latitude using regression analysis for a range of latitude from 8°N to 35°N and operating hours from half an hour to 2.5 hours after sunrise and is given as:

$$\frac{L_{sp\_EW}}{D} = 2.846\phi^{0.133}t^{-0.976} \qquad \text{(eq. 22)}$$

The deviation is found to be within the range of ±10%.

The variation of the spacing in north-south direction is shown in Fig. 9. For latitudes 8°N and 35°N spacing distance in north-south direction is found to be 1.17 D and 1.91 D of the dish respectively. The generalized relationship has been developed for spacing distance between the dishes in north-south direction as function of latitude ranging from 8°N to 35°N by regression analysis and is given by:

$$\frac{L_{sp\_NS}}{D} = 0.0007\phi^2 - 0.0038\phi + 1.1637 \qquad \text{(eq. 23)}$$

and the coefficient of correlation for the above relationship is 0.99.

The variation of the land use factor (LUF) with latitude for various operating hours is shown in Fig. 10. The LUF is found to be 11.55 (8.7% of total land) for 8°N, and 22.89 (4.4% of the total land) 35°N, operating from the half an hour after the sunrise to half an hour before sunset, whereas for same latitudes dish operating from 2.5 hours after the sunrise to 2.5 hours before sunset, the LUF is found to be 2.47 (40.4 % of total land) and 4.79 (20.9 % of the total land) respectively.

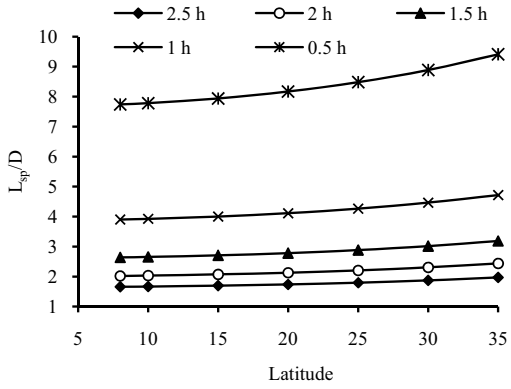

Fig. 8: Spacing distance required between the dishes in east-west direction after different hours after the sunrise

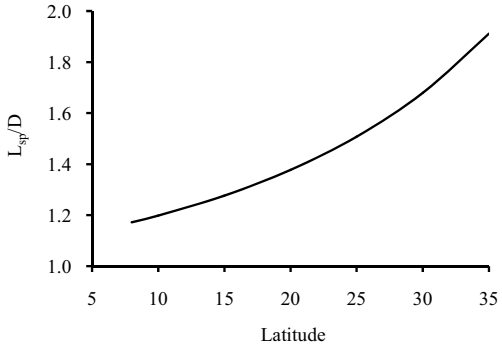

Fig. 9: Spacing distance required between the dishes in north-south at noon on declination -23.45°

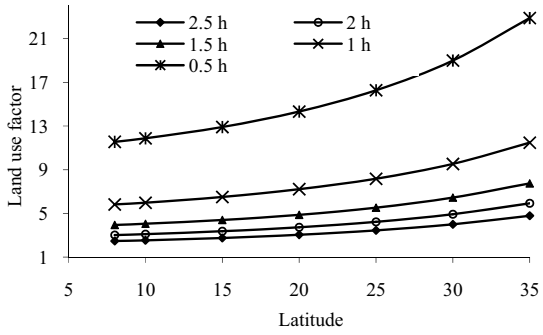

Fig. 10: Land use factor after various hours after/before the sunrise/sunset keeping the spacing distance equal to shadow length at same hours for various latitudes

3.3 Shadow effect on the adjacent dishes

The shadow of reference dish on the adjacent dishes is illustrated in Fig. 11 for latitudes 8°N and 35°N spacing equal to shadow length at 2.5 hours after sunrise and operating 1 hour after sunrise to 1 hour before sunset. The reference dish (D_R) may cast the shadow on the two or three adjacent dishes on different days in a year. The dish (D_R) may cast the shadow on one dish or two dishes simultaneously or some times there will not be any shadow on any of the dishes depending upon the operating hours, spacing distance, latitudes and declination. At the same time, dish (D_R) will experience equal of size of the shadow by opposite dish/dishes. The variation of the percentage shadow falling on the dish for different declination, operating at various operating hours after sunrise to before sunset, when spacing distance equal to shadow length at 2.5 hours after sunrise at the places of latitudes 8°N and 35°N is shown in Fig.12. At higher latitude, the range of percentage variation of the shadow for the different declinations is more as compared to lower latitude places. The average value of the percentage of the shadow is more at lower latitude as compared to higher latitude places.

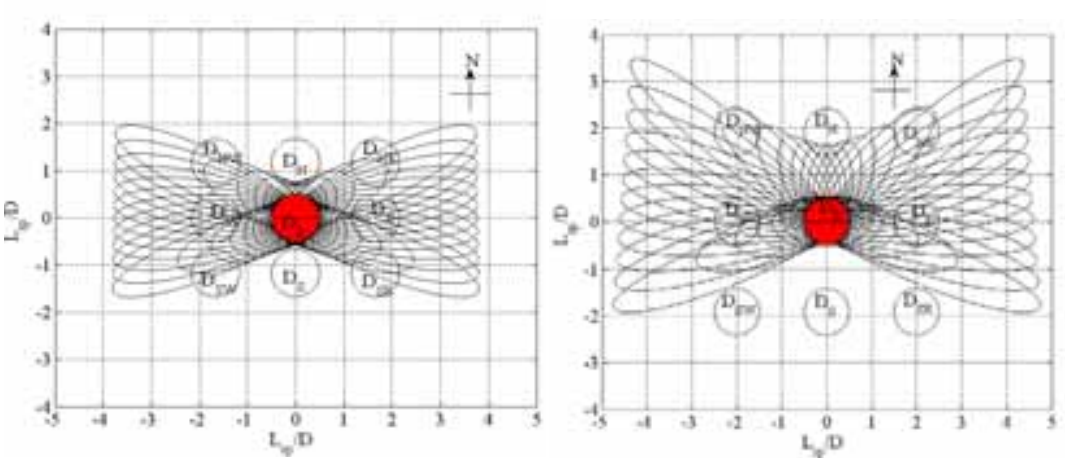

(a) (b)

Fig. 11; Shadow falling on the adjacent dish operating from 1h after sunrise to 1h before sunset and spacing distance at 2.5 h after sunrise at latitudes (a) 8°N and (b) 35°N

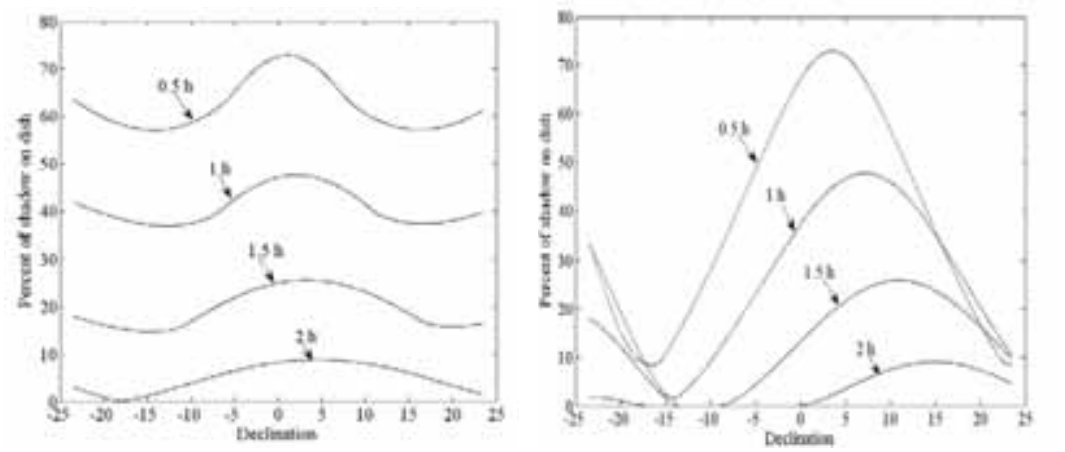

(a) (b)

Fig. 12: Percentage of shadow falling on the dish operating at various hours keeping spacing distance at 2.5h after sunrise at latitudes (a) 8°N and (b) 35°N

4. Conclusions

The variation in the image length and image area on the receiver was studied as a function of rim angle of the solar dish. Rim angle between 40^{o} to 50^{o} was found to be ideal as it gives small concentrated images. The shadow profile around the dish throughout the year at various latitudes (8°N-35°N) in India for various plant-operating hours is determined. In-line arrangement of the solar dish collector arrays is found to be a better choice in terms of the minimum land area required for setting up the power plant. The variation of the percentage shadow falling on the dish for different declination, operating at various operating hours after sunrise to before sunset was studied. It was observed that at higher latitude, the range of percentage variation of the shadow for the different declinations is more as compared to lower latitude places. The average value of percentage of the shadow is more at lower latitude as compared to higher latitude places.

Nomenclature

a	semi major axis length of the elliptical images (m)	θ_s	sun aperture angle (32')
A	area (m^2)	δ	declination angle (deg)
b	semi minor axis length of the elliptical images (m)	ϕ	latitude angle (deg)
D	aperture diameter of the dish (m)	ω	hour angle (deg)
f	focal length(m)	**Subscript**	
L	length (m)	EW	east-west direction
LUF	land use factor	NS	north-south direction
t	operating time (hours)	i	image
x,y	cartesian coordinates	p	aperture
Greek symbols		sh	shading
α	altitude angle (deg)	sp	spacing
β	reflector title angle(deg)	sr	sunrise
γ	azimuth angle (deg)	ss	sunset
θ	rim angle (deg)	s	sun or solar
θ_r	reflected ray angle (deg)	r	reflection

References

Aparporn S., Somchai K., 2007. Solar flux distribution on a cylindrical receiver surface of a central receiver system. Solar Energy, 2, 27-29.

Appelbaum J. and Bany J., 1979. Shadow effect of adjacent solar collectors in large scale systems. Solar Energy, 23, 497–507.

Aronova, E.S., Grilikhes, V.A., Shvarts, M.Z., 2008. Optimization of arrangement of photoelectric power plants with radiation concentrators in solar electric power plant design. Applied Solar Energy, 44 (4), 237–242.

Barra, O., Conti, M., Santamata, E., Scarmozzino, R., Visentin, R., 1977. Shadow effect in a large scale solar power plant. Solar Energy, 19(6), 759-762.

Groumpos, P.P., Khouzam, K., 1987. A generic approach to the shadow effect of large solar power systems. Solar Cells, 22 (1), 29-46.

Jeter, S. M., 1986. The distribution of concentrated solar radiation in paraboloidal collector. Solar Energy Engineering, 108, 219-225.

Kaushika N.D., 1993. Viability aspects of paraboloidal dish solar collector systems. Renewable Energy, 3(6-7), 87-93.

Kaushika N.D. and Reddy K.S., 2000. Performance of a low cost solar paraboloidal dish steam generating system. Energy Conversion Management, 41, 713-726.

Liul, Y.,. Dai1 J. M., Sun X. G., Yu T.H., 2003. Factors influencing on flux distribution on focal region of parabolic concentrators. Journal of Physics, 48, 59–63.

Reddy K.S. and Kumar N.S., 2005. Performance evaluation of cavity receivers for fuzzy focal solar dish concentrator, International Congress on Renewable Energy -2005, Hotel Le-Meridian, Pune, 396 - 410.

Reddy K.S. and Veershetty G., 2009. Flux distribution of 20 m^2 fuzzy focal solar parabolic dish concentrator. International Conference on 'Advances in Energy Research' (ICAER) 2009, IIT Bombay, 386-391.

Robert D. L. R., Eugene Jr. L E., Joel B. L., Hester K. N., 1957. Flux near the focal plane. Solar Energy, 1, 2-3.